

(PT）-symmetry phase transition in a bipartite lattice with long-range interactions

Dapeng Zheng(郑大鹏), Siwu Li(李思吾), and Zeliang Xiang(项泽亮)
Citation: Chin. Phys. B, 2025, 34 (**11**): 110305. DOI: 10.1088/1674-1056/addcd4
http://cpb.iphy.ac.cn; http://iopscience.iop.org/cpb

What follows is a list of articles you may be interested in

Antichiral edge states in a square lattice

Peng-Yu Guo(郭鹏宇), Wei Li(黎炜), Junhui Hu(胡君辉), and Hai-Xiao Wang(王海啸)
Chin. Phys. B, 2025, 34 (**10**): 100307. DOI: 10.1088/1674-1056/add90c

Non-quantized Zak phases, PT/APT symmetry transitions, and doubly degenerate exceptional points in a non-Hermitian spin-orbit coupled SSH model

Jun-Xing Huo(霍俊行), Jian Li(李健), Qing-Xu Li(李清旭), and Jia-Ji Zhu(朱家骥)
Chin. Phys. B, 2025, 34 (**7**): 070301. DOI: 10.1088/1674-1056/adc7f3

Ground state of SU(3) spin-orbit coupled soft-core Bose gas

Jia Liu(刘佳), Jing Feng(冯婧), Ya-Jun Wang(王雅君), Xiao-Fei Zhang(张晓斐), and Xue-Ying Yang(杨雪滢)
Chin. Phys. B, 2025, 34 (**6**): 060301. DOI: 10.1088/1674-1056/adc36b

Asymmetric mode-pairing quantum key distribution with advantage distillation

Hai-Tao Wang(汪海涛), Chun Zhou(周淳), Yi-Fei Lu(陆宜飞), Chen-Peng Hao(郝辰鹏), Yan-Mei Zhao(赵燕美), Yan-Yang Zhou(周砚扬), Hong-Wei Li(李宏伟), and Wan-Su Bao(鲍皖苏)
Chin. Phys. B, 2025, 34 (**4**): 040305. DOI: 10.1088/1674-1056/adbb5c

Quantum manipulation of asymmetric Einstein-Podolsky-Rosen steering in controllable dynamical Casimir arrays

Ruinian Li(李瑞年), Yumei Long(龙玉梅), and Xue Zhang(张雪)
Chin. Phys. B, 2025, 34 (**2**): 020307. DOI: 10.1088/1674-1056/ad9a99

$\mathcal{PT}$-symmetry phase transition in a bipartite lattice with long-range interactions

Dapeng Zheng(郑大鹏), Siwu Li(李思吾), and Zeliang Xiang(项泽亮)†

School of Physics, Sun Yat-sen University, Guangzhou 510275, *China*

(Received 10 April 2025; revised manuscript received 23 May 2025; accepted manuscript online 26 May 2025)

We investigate the parity–time ($\mathcal{PT}$) symmetry-breaking quantum phase transition in a one-dimensional (1D) bosonic lattice featuring cavity-mediated long-range interactions and spatially staggered dissipation. By mapping the system to an effective spin chain under the constraints of hard-core bosons and integrating the mean-field decoupling approach with biorthogonal basis formalism, we derive a self-consistency equation. Numerical simulation results validate that the derived equation quantitatively captures the $\mathcal{PT}$-symmetry order parameter's phase diagram. Our findings reveal that coherent hopping maintains $\mathcal{PT}$ symmetry through quantum fluctuations. Conversely, cavity-engineered long-range interactions, in synergy with staggered dissipation, act in opposition to drive symmetry breaking. This competitive interplay can inspire further exploration of tunable quantum phase transitions in non-Hermitian systems.

Keywords: $\mathcal{PT}$ symmetry, 1D bosonic lattice, long-range interactions, staggered dissipation, quantum phase transition

PACS: 03.65.Yz, 42.50.Pq, 64.70.Tg, 05.30.Jp

DOI: 10.1088/1674-1056/addcd4 **CSTR:** 32038.14.CPB.addcd4

1. Introduction

Ultracold atoms in optical lattices provide an experimentally accessible quantum platform for simulating strongly interacting many-body systems and exploring fundamental quantum phases with precise control of interactions and lattice configurations.[1–6] This platform has become a paradigmatic realization of the Bose–Hubbard (BH) model, successfully emulating equilibrium phenomena including the Mott insulator (MI) to superfluid (SF) transition.[7–12] Early studies on this field were predominantly confined to closed quantum systems with short-range couplings due to experimental limitations, whereas state-of-the-art precision control techniques have now enabled two transformative capabilities: controlled dissipation for stabilizing non-equilibrium quantum states,[13–15] and tunable long-range interactions mediated by optical cavities.[16–20] These developments enable the realization of novel phases, such as the supersolids (SS) and the charge density waves (CDW).[21–25]

Recent breakthroughs in dissipative cold-atom platforms have enabled the creation of synthetic gain-loss landscapes exhibiting parity–time ($\mathcal{PT}$) symmetry.[26–31] In the context of non-Hermitian quantum mechanics and open quantum systems, two particular symmetries are of relevance: parity ($\mathcal{P}$) symmetry, or spatial inversion, and time-reversal ($\mathcal{T}$) symmetry. If the action of the combined $\mathcal{PT}$ operators on the Hamiltonian satisfies the relation $\mathcal{PT}H(\mathcal{PT})^{-1} = H$, the Hamiltonian is $\mathcal{PT}$-symmetric.[32–34] In these systems, balanced non-Hermitian potentials preserve real energy spectra until spontaneous $\mathcal{PT}$-symmetry breaking occurs, triggering a transition to complex eigenvalues, which is a hallmark of non-Hermitian criticality.[32,35] State-of-the-art studies employing complementary theoretical approaches, including mean-field approximations, analytically exact methods, and nonlinear spin-wave theory, have systematically identified distinct phenomena in one-dimensional (1D) $\mathcal{PT}$-symmetric quantum systems: the collapse of quantum–classical correspondence,[36] topological boundary-induced spectral reconstruction,[37] and emergent dynamical instability mechanisms.[38] At the same time, coupling atoms to high-finesse optical cavities enables photon-mediated long-range interactions[16,17] where atoms coherently exchange photons over extended lattice distances. This kind of experimental setup was successfully established in Ref. [23], which achieved independent control over three energy scales by combining an optical lattice with cavity-mediated interactions and observed the presence of SS and CDW phases.

Emerging theoretical and experimental advances have unveiled a variety of $\mathcal{PT}$-symmetry breaking phenomena and unconventional collective phases in non-Hermitian quantum systems with long-range interactions.[39–43] Notable experimental breakthroughs in optically coupled nanoparticle arrays[39] and trapped-ion platforms[40] have successfully realized non-Hermitian dynamics with precisely controlled exceptional points. From a theoretical perspective, the synergy between dissipative processes and long-range coupling has been shown to induce novel quantum phases and funda-

†Corresponding author. E-mail: xiangzliang@mail.sysu.edu.cn

© 2025 Chinese Physical Society and IOP Publishing Ltd. All rights, including for text and data mining, AI training, and similar technologies, are reserved.

mentally modify entanglement scaling laws in extended spin systems.[41–43] These findings collectively underscore the critical importance of investigating the intertwined effects of non-Hermiticity and long-range interactions in quantum many-body physics. Since non-Hermitian dissipation and long-range interactions inherently disrupt the spatial symmetry required for $\mathcal{PT}$-symmetry, whereas coherent hopping tends to preserve it,[20,35] elucidating the competition between these mechanisms is essential for understanding quantum phase transitions in non-equilibrium systems.[44,45]

In this work, we focus on the effects of cavity-mediated interactions on bosons in a 1D bipartite optical lattice with alternating gain and loss. The system maintains $\mathcal{PT}$ symmetry when coherent hopping and long-range interactions are balanced, while symmetry breaking emerges at critical hopping strengths. We demonstrate that for hard-core bosons (*i.e.*, strong on-site repulsion that allows only single-particle occupancy) in one dimension, the phase diagram of the effective ground state characterized by the lowest real part of the eigenspectrum[46] is influenced by all of hopping, dissipation, and interactions. These effects combine in a non-trivial manner, resulting in a complex phase diagram that extends beyond the traditional MI to SF transition. We show that the interplay between $\mathcal{PT}$-preserving quantum fluctuations (dominated by hopping) and $\mathcal{PT}$-breaking mechanisms, cavity-mediated long-range interactions as well as dissipation, leads to a dynamic competition. This redefinition of quantum criticality in open systems provides new insights into phase transitions in non-local interaction and non-Hermitian systems.[47,48]

The rest of the paper is organized as follows. Section 2 introduces the non-Hermitian model and derives its effective Hamiltonian via boson-spin mapping, establishing the foundation for $\mathcal{PT}$-symmetry analysis. Then, in Section 3, we systematically develop the self-consistency equation using the biorthogonal basis formulation, which enables Section 4 to construct the phase diagram and analyze the factors that dominate the phase transition. Finally, we summarize the main results in Section 5.

2. Model

Bosons in an optical lattice with cavity-mediated long-range interactions are described by an extended Bose–Hubbard (EBH) model.[16,49–52] We consider an ensemble of bosonic gas trapped in a 1D optical lattice located inside an optical cavity, and its dynamics can be described by the Hamiltonian[25]

$$\hat{H} = -t\sum_j \left(\hat{b}_j^\dagger \hat{b}_{j+1} + \text{H.c.}\right) - \mu\sum_j \hat{n}_j + \frac{U_0}{2}\sum_j \hat{n}_j(\hat{n}_j - 1) + \frac{U_1}{N}\left(\sum_{j\in \text{e}} \hat{n}_j - \sum_{j\in \text{o}} \hat{n}_j\right)^2, \quad (1)$$

where $\hat{b}_j^\dagger$ ($\hat{b}_j$) is the bosonic creation (annihilation) operator at the j-th site, $\hat{n}_j = \hat{b}_j^\dagger \hat{b}_j$ is the number operator, N is the number of sites, t is the tunneling amplitude, U_0 is the on-site repulsion, μ is the chemical potential, and U_1 is the strength of the infinite-range interactions mediated by the cavity. The first line in Eq. (1) represents the single-particle part of the atomic gases, while the second line describes both local and global-range interactions in the system. The cavity-mediated long-range interactions are represented as the square of the density-wave order parameter $\hat{x}$,

$$\hat{x} = \sum_{j\in \text{e}} \hat{n}_j^z - \sum_{j\in \text{o}} \hat{n}_j^z, \quad (2)$$

where $\sum_{j\in \text{e}}$ ($\sum_{j\in \text{o}}$) represents the sum over even (odd) lattice sites.[45]

In the hard-core boson limit ($U_0 \to \infty$), onsite multiple occupancy is strictly prohibited, thereby mapping the system to spin-1/2 excitations with single-particle per site constraints. The mapping is given by $\hat{b}_j^\dagger \to \hat{S}_j^\dagger = \hat{S}_j^x + \mathrm{i}\hat{S}_j^y$ and $\hat{b}_j^\dagger \hat{b}_j \to \hat{S}_j^z + 1/2$,[53] which allows us to obtain an effective 1D-spin-chain model for the system, as shown in Fig. 1,

$$\hat{H}_{\text{spin}} = -t\sum_j \left(\hat{S}_j^+ \hat{S}_{j+1}^- + \text{H.c.}\right) - \mu\sum_j \left(\hat{S}_j^z + \frac{1}{2}\right) + \frac{U_1}{N}\left(\sum_{j\in \text{e}} \hat{S}_j^z - \sum_{j\in \text{o}} \hat{S}_j^z\right)^2. \quad (3)$$

The density-wave order parameter corresponds to the lattice's total staggered magnetization, which quantifies antiferromagnetic long-range order. We can define it as

$$\hat{M} = \sum_{j\in \text{e}} \hat{S}_j^z - \sum_{j\in \text{o}} \hat{S}_j^z. \quad (4)$$

In the hard-core limit, the cavity-mediated long-range interaction is equivalent to the long-range interaction among the spin-z component. On the other hand, the hopping term in Eq. (1) translates into a ferromagnetic (FM) short-range interaction in the spin-XY plane. Therefore, CDW or SF order in the bosonic system is equivalent to AFM-z or FM-xy order in the spin system.[25]

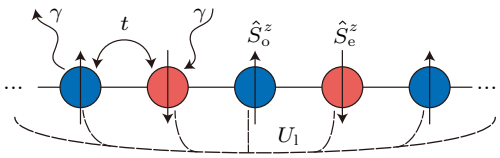


Fig. 1. Schematic diagram of the 1D spin chain model.

Previous analysis has predominantly focused on the Hermitian sector of the system, with intentional omission of non-Hermitian processes. To extend this model into the non-Hermitian domain, a $\mathcal{PT}$-symmetric configuration is engineered by imposing staggered dissipation: even (odd) lattice

sites experience particle gain (loss) at rate γ, encoded in the Hamiltonian $\hat{H}_{\rm eff} = \hat{H}_{\rm spin} - \frac{{\rm i}\gamma}{2}\sum_j (-1)^j \hat{n}_j$. Here, the alternating sign factor $(-1)^j$ explicitly correlates with the spatial dissipation pattern, preserving the system's $\mathcal{PT}$-symmetry through balanced gain and loss. In our analysis, we focus on the system dynamics within a timescale that is short compared to the inverse loss rate $1/\gamma$. In this case, the eigenstate associated with the lowest real part of the eigenspectrum can be identified as the effective ground state, while the imaginary components of the eigenenergies characterize the decay rates corresponding to each eigenstate.[46] The effective non-Hermitian Hamiltonian can be expressed as

$$\begin{aligned}\hat{H}_{\rm eff} =& -t\sum_j \left(\hat{S}_j^+ \hat{S}_{j+1}^- + {\rm H.c.}\right) - \mu \sum_j \left(\hat{S}_j^z + \frac{1}{2}\right) \\ & - \frac{{\rm i}\gamma}{2}\sum_j (-1)^j \hat{S}_j^z + \frac{U_{\rm l}}{N}\left(\sum_{j\in {\rm e}} \hat{S}_j^z - \sum_{j\in {\rm o}} \hat{S}_j^z\right)^2 \\ =& -t\sum_j \left(\hat{S}_j^+ \hat{S}_{j+1}^- + {\rm H.c.}\right) - \mu \sum_j \left(\hat{S}_j^z + \frac{1}{2}\right) \\ & - \frac{{\rm i}\gamma}{2}\sum_j (-1)^j \hat{S}_j^z + \frac{U_{\rm l}}{N}\sum_{j,k} J_{jk}\hat{S}_j^z \hat{S}_k^z, \end{aligned} \tag{5}$$

where $J_{jk} = (-1)^{j+k}$.

The non-Hermitian Hamiltonian can be studied through a mean-field decoupling scheme. Central to this approach is the order parameter $m \equiv \langle \hat{M} \rangle / N$. Applying the linearization procedure,

$$\hat{M}^2 \approx 2\langle \hat{M} \rangle \hat{M} - \langle \hat{M} \rangle^2, \tag{6}$$

the original quartic interaction is reduced to a linear operator form. Applying the linear approximation to the effective Hamiltonian (5) eliminates explicit operator products, yielding the mean-field form[24]

$$\begin{aligned}\hat{H}_{\rm MF} =& -t\sum_j \left(\hat{S}_j^+ \hat{S}_{j+1}^- + {\rm H.c.}\right) - \mu \sum_j \left(\hat{S}_j^z + \frac{1}{2}\right) \\ & - \frac{{\rm i}\gamma}{2}\sum_j (-1)^j \hat{S}_j^z + 2U_{\rm l} m \hat{M} - U_{\rm l} N m^2. \end{aligned} \tag{7}$$

The self-consistency equation for the imbalance order parameter m can be derived from $m = \langle \hat{M} \rangle / N$.

The spin operators can be mapped to fermionic operators through the Jordan–Wigner transformation. This procedure converts the original interacting spin system into a quadratic fermionic model, which can be exactly solved in one dimension[54–56]

$$\hat{S}_j^+ = \hat{c}_j^\dagger {\rm e}^{{\rm i}\pi \sum_{l<j} \hat{c}_{\rm l}^\dagger \hat{c}_{\rm l}}, \quad \hat{S}_j^z = \hat{c}_j^\dagger \hat{c}_j - \frac{1}{2}. \tag{8}$$

Consequently, the mean-field Hamiltonian in Eq. (7) reduces to a quadratic form in terms of fermionic operators,

$$\begin{aligned}\hat{H}_{\rm MF} =& -t\sum_j \left(\hat{c}_j^\dagger \hat{c}_{j+1} + {\rm H.c.}\right) - \mu \sum_j \hat{c}_j^\dagger \hat{c}_j \\ & - \frac{{\rm i}\gamma}{2}\sum_j (-1)^j \left(\hat{c}_j^\dagger \hat{c}_j - \frac{1}{2}\right) \\ & + 2U_{\rm l} m \sum_j (-1)^j \left(\hat{c}_j^\dagger \hat{c}_j - \frac{1}{2}\right) \\ =& -t\sum_j \left(\hat{c}_j^\dagger \hat{c}_{j+1} + {\rm H.c.}\right) \\ & - \sum_j \left[\mu + (-1)^j \left(\frac{{\rm i}\gamma}{2} + 2U_{\rm l} m\right)\right] \hat{c}_j^\dagger \hat{c}_j. \end{aligned} \tag{9}$$

Note that the constant terms are neglected since they do not change the system's dynamic properties.

3. Self-consistency equation

Following the formulation of the fermionic mean-field Hamiltonian, we can drive the self-consistency equation. Due to the staggered potential terms $(-1)^j$ of the system, the lattice can be divided into even $(j = 2m)$ and odd $(j = 2m+1)$ sublattices. This bipartition is formally implemented by defining sublattice operators,

$$\hat{c}_{2m} = \frac{1}{\sqrt{N/2}}\sum_k {\rm e}^{{\rm i}km} a_k, \quad \hat{c}_{2m+1} = \frac{1}{\sqrt{N/2}}\sum_k {\rm e}^{{\rm i}km} b_k. \tag{10}$$

In momentum space, the Hamiltonian can be written as

$$\hat{H}_{\rm MF} = \sum_k \begin{pmatrix} a_k^\dagger & b_k^\dagger \end{pmatrix} \begin{pmatrix} -\mu - \epsilon_k & \xi_k \\ \xi_k^\dagger & -\mu + \epsilon_k \end{pmatrix} \begin{pmatrix} a_k \\ b_k \end{pmatrix}, \tag{11}$$

in which

$$\epsilon_k = \frac{{\rm i}\gamma}{2} + 2U_{\rm l} m, \quad \xi_k = -2t\cos\left(\frac{k}{2}\right){\rm e}^{-{\rm i}k/2}. \tag{12}$$

Diagonalization of the Hamiltonian matrix yields the eigenenergy spectrum E_k,

$$E_k^\pm = -\mu \pm \sqrt{4t^2\cos^2\left(\frac{k}{2}\right) + \epsilon_k^2}. \tag{13}$$

By employing the sublattice decomposition defined in Eq. (10), the self-consistency equation can be expressed in momentum space as

$$\begin{aligned} m =& \frac{1}{N}\sum_j (-1)^j \left\langle \hat{c}_j^\dagger \hat{c}_j \right\rangle \\ =& \frac{1}{N}\sum_j \left(\left\langle \hat{a}_k^\dagger \hat{a}_k \right\rangle - \left\langle \hat{b}_k^\dagger \hat{b}_k \right\rangle\right). \end{aligned} \tag{14}$$

In the thermodynamic limit $(N \to \infty)$, the sum can be converted into an integral

$$m = \int_{-\pi}^{\pi} \frac{{\rm d}k}{2\pi} \left(\left\langle \hat{a}_k^\dagger \hat{a}_k \right\rangle - \left\langle \hat{b}_k^\dagger \hat{b}_k \right\rangle\right). \tag{15}$$

The derivation of the exact self-consistency equation requires computing the particle density difference between sublattices $\langle \hat{a}_j^\dagger \hat{a}_j \rangle$ and $\langle \hat{b}_j^\dagger \hat{b}_j \rangle$. In our model at effective zero

temperature,[46] when the chemical potential is set to $\mu = 0$, the negative energy eigenstates E_k^- are completely occupied, while the positive energy eigenstates E_k^+ remain unoccupied.

The Bogoliubov transformation provides a systematic framework for calculating quantum expectation values.[57] In non-Hermitian systems, the Bogoliubov transformation requires extension to a biorthogonal basis to preserve canonical relations.[58] Defining right ($|\Psi_R\rangle$) and left ($|\Psi_L\rangle$) eigenstates with $\langle\Psi_L|\Psi_R\rangle = 1$, the dual transformations are

$$\begin{pmatrix} a_k \\ b_k \end{pmatrix} = M_R \begin{pmatrix} \gamma_k \\ \eta_k \end{pmatrix}, \quad \begin{pmatrix} a_k^\dagger \\ b_k^\dagger \end{pmatrix}^T = \begin{pmatrix} \gamma_k^\dagger \\ \eta_k^\dagger \end{pmatrix}^T M_L, \tag{16}$$

where the biorthogonal matrices $M_R = \begin{pmatrix} u_k^R & v_k^R \\ w_k^R & z_k^R \end{pmatrix}$ and $M_L = \begin{pmatrix} u_k^R & v_k^R \\ w_k^R & z_k^R \end{pmatrix}$ satisfy $M_R M_L = I$.

The conventional definition of the order parameter becomes inadequate in non-Hermitian systems due to the non-orthogonality of the eigenstates. To maintain thermodynamic consistency, the order parameter must be redefined in the biorthogonal basis as

$$m = \frac{\langle\Psi_L|\hat{M}|\Psi_R\rangle}{N\langle\Psi_L|\Psi_R\rangle}. \tag{17}$$

The fermionic operators expand in terms of quasiparticles as

$$a_k^\dagger a_k = (u_k^R\gamma_k^\dagger + w_k^R\eta_k^\dagger)(u_k^R\gamma_k + v_k^R\eta_k), \tag{18}$$
$$b_k^\dagger b_k = (v_k^R\gamma_k^\dagger + z_k^R\eta_k^\dagger)(w_k^R\gamma_k + z_k^R\eta_k). \tag{19}$$

Calculating the biorthogonal transformation coefficients, we get

$$\left\langle \hat{a}_j^\dagger \hat{a}_j \right\rangle - \left\langle \hat{b}_j^\dagger \hat{b}_j \right\rangle = -\frac{|\xi_k|^2 - |\epsilon_k + \Delta_k|^2}{|\xi_k|^2 + |\epsilon_k + \Delta_k|^2} \cdot \Theta\left(-\mathrm{Re}\left(E_k^-\right)\right), \tag{20}$$

where $\Delta_k = \sqrt{4t^2\cos^2(k/2) + \epsilon_k^2}$. Through this relation, we can obtain the self-consistency equation,

$$m = -\int_{-\pi}^{\pi} \frac{|\xi_k|^2 - |\epsilon_k + \Delta_k|^2}{|\xi_k|^2 + |\epsilon_k + \Delta_k|^2} \cdot \Theta\left(-\mathrm{Re}\left(E_k^-\right)\right) \frac{\mathrm{d}k}{2\pi}. \tag{21}$$

In this equation, the Heaviside step function $\Theta(\cdot)$ restricts the integration domain to the negative-energy states, ensuring that only these states exclusively contribute to the order parameter. Since the origin of dissipation can introduce a non-Hermitian term in the energy spectrum, the real part of E_k^- is used to avoid complex-valued outputs in step functions, ensuring physically meaningful results. Having derived the general form of the self-consistency equation, we now turn to a systematic analysis of its mathematical structure and physical implications.

Prior to mathematical analysis, qualitative insights emerge. We first examine the non-interacting case with $U_l = 0$, where the solution to the self-consistency equation reduces to the trivial configuration $m_0 = 0$. Through rigorous analysis of the energy spectrum given in Eq. (13), the critical parameter for $\mathcal{PT}$-symmetry breaking is explicitly determined as $t_c = \gamma/4$. This critical threshold marks the emergence of complex eigenvalues in the spectrum, characterizing the phase transition to a fully $\mathcal{PT}$-symmetry broken phase with order parameter $|m| = 1$.

When $U_l \neq 0$, long-range interactions modify both the energy spectrum Eq. (13) and the self-consistency equation (21), thereby precluding analytical solutions. We numerically solve this equation through iterative computation of the order parameter m, systematically mapping how U_l-controlled interactions select distinct quantum phases.

For positive interaction strength, $U_l > 0$, the system stabilizes a paramagnetic phase with strict sublattice spin balance $m = 0$, where long-range interaction energies vanish identically. Under these conditions, the energy contribution from the long-range interaction term vanishes identically. Conversely, negative interaction strength, $U_l < 0$, drives spontaneous symmetry breaking $m \neq 0$, inducing a sublattice-ordered phase with antiferromagnetic-type alignment. This ordering features magnetization contrast between parity-opposite sublattices, resulting in long-range spin correlations.

At $t = 0$, spin dynamics become confined to the XY-plane with suppressed hopping. In this frozen limit, the system exhibits sharp solutions: $m = 0$ for $U_l > 0$ and $m = 1$ for $U_l < 0$. The hopping amplitude t activates quantum fluctuations through the kinetic term, which progressively suppresses long-range order and drives a quantum phase transition to a gapless spin liquid state when t surpasses the critical value t_c,[59] with the ordered phase persisting only when $t < t_c$.

4. Phase diagram

In this section, we perform numerical simulations across the parameter space to validate the solutions from the self-consistency equation. Figure 2(a) demonstrates the phase diagram of Eq. (5) obtained through exact diagonalization (ED) implemented within the biorthogonal basis framework. The criticality at $U_l = 0$ manifests as a phase transition where the order parameter m vanishes for $U_l > 0$ while attains finite values under attraction $U_l < 0$ at small t, indicating spontaneous $\mathcal{PT}$-symmetry breaking. Notably, singularities emerge at the parameter boundaries $\gamma = 0$, which merit explicit physical interpretation. As shown in Fig. 2(b), solutions to the self-consistency equation (Eq. (21)) maintain quantitative agreement with ED across the parameter space, despite localized discrepancies near the $\gamma = 0$ boundary. The amplified $\mathcal{PT}$-symmetry breaking observed in ED data, characterized by en-

hanced m values compared to predictions, will be analyzed in the following content.

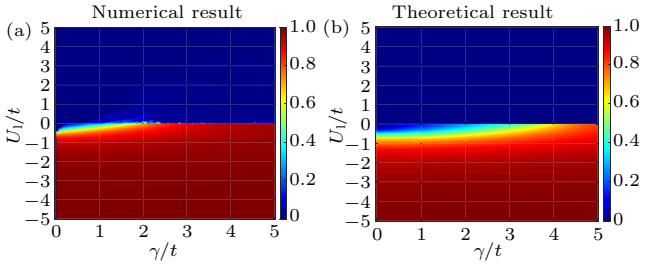


Fig. 2. (a) Biorthogonal exact diagonalization of Eq. (5) for a 12-site system, (b) two-dimensional (2D) parametric sweep of solutions to self-consistency equation (21). The color bar represents the absolute value of m.

At $\gamma = 0$, the order parameter m vanishes across the entire parameter space, which is a manifestation of finite-size effects inherent to ED methods.[60] The ground state manifests as a quantum superposition of two degenerate Néel configurations: $|\Psi_{\rm GS}\rangle = (1/\sqrt{2})(|\uparrow\downarrow\uparrow\downarrow\cdots\rangle + |\downarrow\uparrow\downarrow\uparrow\cdots\rangle)$, which symmetrizes the staggered magnetization and enforces $m = \langle\hat{M}\rangle/N = 0$. The hidden order parameter is quantified via the staggered magnetization variance[61,62]

$$v(N) = \frac{\sqrt{\left(\langle\hat{M}^2\rangle - \langle\hat{M}\rangle^2\right)}}{N} \quad (N = 4, 6, \ldots, 16), \tag{22}$$

with thermodynamic extrapolation implemented through the scaling relation,

$$v(N) = v(\infty) + \frac{a}{N} + \frac{b}{N^2}, \tag{23}$$

as detailed in Fig. 3(a). The non-zero extrapolated order parameter $v(\infty)$ definitively establishes long-range ordering in the thermodynamic limit, even though m vanishes in finite-size ED calculations.

The system exhibits a clear phase transition between the spin-liquid and antiferromagnetic phases when $U_l < 0$, as per our expectations. This critical behavior demonstrates quantitative agreement with the numerical solutions of the self-consistency equation shown in Fig. 3(b), confirming the consistency of our analytical framework.

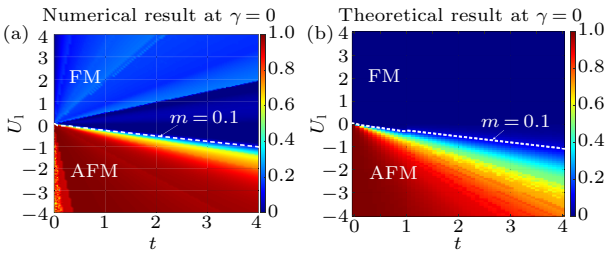


Fig. 3. (a) Thermodynamic-limit behavior of the staggered magnetization variance v_∞ in the absence of dissipation. Finite v values at $U_l > 0$ arise from the numerical extrapolation method. (b) The solution of the self-consistency equation at vanishing dissipation strength $\gamma = 0$. The white dashed line marks the $m = 0.1$ contour, and the color bar represents the absolute value of m.

To systematically map the phase diagram, we show the dependence of the order parameter m on U_l/t at fixed γ/t, as well as its dependence on γ/t at fixed U_l/t. As seen in Fig. 4, $|m|$ remains zero for $U_l > 0$, while for $U_l < 0$, $|m|$ exhibits a discontinuous jump to a value between 0 and 1, which increases with larger γ/t. Overall, there is good agreement between the theoretical predictions and the numerical results, although discrepancies between theory and exact diagonalization (ED) data are also evident. The nonzero values of $|m|$ for $U_l > 0$ in the ED results are likely attributable to finite-size effects, since $|m|$ is expected to vanish in the thermodynamic limit. Similarly, the vanishing of $|m|$ at small γ/t for $U_l < 0$ may also arise from finite-size limitations. Furthermore, we perform cross-sectional scans through the (γ, t, U_l) parameter space, as shown in Fig. 5. The critical hopping strength $t_c = \gamma/4$ at $\gamma = 2.5$ is marked by white dashed lines, serving as a reference for a symmetry-breaking threshold. An analysis of the $\mathcal{PT}$-symmetry properties' dependence on U_l reveals that for $U_l < 0$, increasing $|U_l|$ correlates with higher t_c, indicating a stronger tendency for spontaneous $\mathcal{PT}$-symmetry breaking. The $m = 0.5$ contour (black dashed lines) is overlaid to highlight discrepancies between the ED results and theoretical predictions. Note that this contour does not correspond to the critical boundary between the $\mathcal{PT}$-symmetry and broken phases.

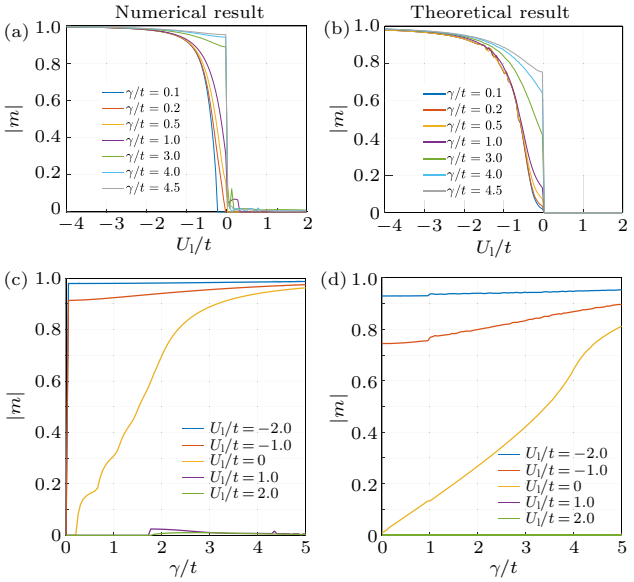


Fig. 4. Comparisons of the ED results (left column) and theoretical results (right column) for the order parameter $|m|$ as a function of varying parameters. Left panels (a) and (c) display numerical results, while right panels (b) and (d) show the corresponding theoretical predictions. Panels (a) and (b) correspond to fixed γ/t, whereas panels (c) and (d) correspond to fixed U_l/t. Different colors indicate different parameter values, with the specific mappings shown in the inset.

A notable feature in both Figs. 4 and 5 is the pronounced enhancement of $\mathcal{PT}$-symmetry breaking, as revealed by the ED results. This enhancement originates from two key factors in our non-Hermitian ED implementation. (i) The open-boundary condition induces wavefunction localization via the non-Hermitian skin effect, amplifying boundary-state contributions to m. (ii) Finite-size effects produce quasi-degenerate

energy levels that prevent complete gap closure near the phase transition, enabling preemptive order parameter growth. Particularly, our approach, which assumes spatially uniform order parameters and inherently smooths finite-size fluctuations through thermodynamic-limit derivation, underestimates boundary localization contributions to m.

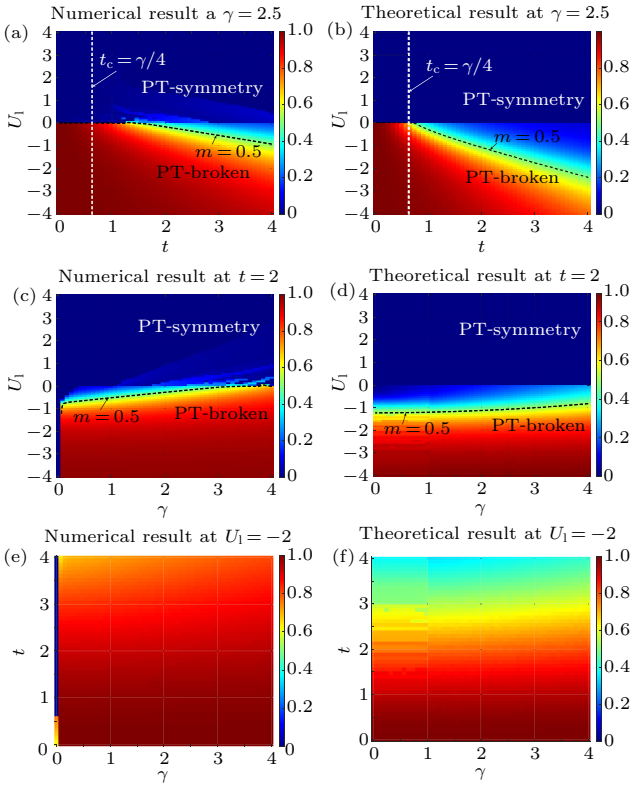


Fig. 5. Comparisons between the results of ED (left column) and solutions to self-consistency equation (right column) at $\gamma = 2.5$, $t = 2$, and $U_l = -2$. Left panels (a), (c), (e) show numerical results, while right panels (b), (d), (f) correspond to theoretical predictions, respectively. In panels (a) and (b), the white dashed lines indicate the critical parameter $t_c = \gamma/4$, while the black dashed lines correspond to the $m = 0.5$ contour. Similarly, the color bar denotes the absolute value of m.

The global trend reveals competing mechanisms: Parameters γ and U_l drive bosons toward odd–even symmetry breaking (spatially modulated distribution), thereby enhancing m and promoting $\mathcal{PT}$-symmetry breaking. In contrast, hopping strength t amplifies quantum fluctuations that homogenize boson distribution and preserve $\mathcal{PT}$ symmetry. This is the same as what we obtained from our qualitative analysis from an energy perspective. Furthermore, the quantitative consistency between theoretical predictions from the self-consistency equation and numerical simulations across all parameter regimes (γ, t, U_l) within mean-field error margins demonstrates the validity of the theoretical framework of the biorthogonal basis.

5. Conclusions

Our analysis reveals that the $\mathcal{PT}$-symmetry breaking in a 1D bosonic lattice arises exclusively from the interplay between dissipation (staggered gain-loss) and long-range interactions, while the hopping terms preserve $\mathcal{PT}$-symmetry. The $\mathcal{PT}$-broken phase emerges only in the attractive interaction regime, where cavity-induced long-range correlations amplify density imbalances. Dissipation extends the parameter regime of $\mathcal{PT}$-symmetry breaking to higher hopping amplitudes, and the non-Hermitian gain-loss modulation amplifies the symmetry breaking. The synergy between $\mathcal{PT}$-symmetric dissipation and cavity-mediated engineering may host emergent topological edge modes and non-Hermitian skin effects and construct a tunable platform for controlling dissipative phases, probing exotic quantum transport phenomena, and developing fault-tolerant quantum sensors. In addition, we observe noticeable discrepancies between the ED results and theoretical predictions. To resolve these differences and to enable more accurate comparisons, further calculations using methods such as DMRG, which can handle larger system sizes, are warranted.

These findings not only highlight the crucial roles of long-range interactions and dissipation in $\mathcal{PT}$-symmetry breaking, but also open up new avenues for exploration in related fields. For example, the insights gained from this work may inspire further research into $\mathcal{PT}$-symmetric engineering in acoustic metamaterials,[63] quantum magnetism in multicomponent Bose gases in optical lattices,[64] and nonequilibrium phenomena in high-band Bose–Einstein condensates.[65]

Acknowledgement

Project supported by the National Natural Science Foundation of China (Grant No. 12375025).

References

[1] Jaksch D, Bruder C, Cirac J I, Gardiner C W and Zoller P 1998 *Phys. Rev. Lett.* **81** 3108
[2] Bloch I, Dalibard J and Zwerger W 2008 *Rev. Mod. Phys.* **80** 885
[3] Lewenstein M, Sanpera A and Ahufinger V 2012 *Ultracold Atoms in Optical Lattices* (Oxford University Press)
[4] Eckardt A 2017 *Rev. Mod. Phys.* **89** 011004
[5] Gross C and Bloch I 2017 *Science* **357** 995
[6] Schäfer F, Fukuhara T, Sugawa S, Takasu Y and Takahashi Y 2020 *Nat. Rev. Phys.* **2** 411
[7] Fisher M P A, Weichman P B, Grinstein G and Fisher D S 1989 *Phys. Rev. B* **40** 546
[8] Freericks J K and Monien H 1994 *Europhys. Lett.* **26** 545
[9] Kühner T D and Monien H 1998 *Phys. Rev. B* **58** R14741
[10] Greiner M, Mandel O, Esslinger T, Hänsch T W and Bloch I 2002 *Nature* **415** 39
[11] Bakr W S, Peng A, Tai M E, Ma R, Simon J, Gillen J I, Fölling S, Pollet L and Greiner M 2010 *Science* **329** 547
[12] Cazalilla M A, Citro R, Giamarchi T, Orignac E and Rigol M 2011 *Rev. Mod. Phys.* **83** 1405
[13] Breuer H P and Petruccione F 2007 *The Theory of Open Quantum Systems* (Oxford University Press)
[14] Diehl S, Micheli A, Kantian A, Kraus B, Büchler H P and Zoller P 2008 *Nat. Phys.* **4** 878
[15] Hannukainen J and Larson J 2018 *Phys. Rev. A* **98** 042113
[16] Maschler C and Ritsch H 2005 *Phys. Rev. Lett.* **95** 260401
[17] Maschler C, Mekhov I B and Ritsch H 2008 *Eur. Phys. J. D* **46** 545
[18] Ritsch H, Domokos P, Brennecke F and Esslinger T 2013 *Rev. Mod. Phys.* **85** 553
[19] Habibian H, Winter A, Paganelli S, Rieger H and Morigi G 2013 *Phys. Rev. Lett.* **110** 075304

[20] Mivehvar F, Piazza F, Donner T and Ritsch H 2021 *Adv. Phys.* **70** 1

[21] Jaksch D and Zoller P 2005 *Ann. Phys.* **315** 52

[22] Lewenstein M, Sanpera A, Ahufinger V, Damski B, SenDe A and Sen U 2007 *Adv. Phys.* **56** 243

[23] Landig R, Hruby L, Dogra N, Landini M, Mottl R, Donner T and Esslinger T 2016 *Nature* **532** 476

[24] Dogra N, Brennecke F, Huber S D and Donner T 2016 *Phys. Rev. A* **94** 023632

[25] Niederle A E, Morigi G and Rieger H 2016 *Phys. Rev. A* **94** 033607

[26] Guo A, Salamo G J, Duchesne D, Morandotti R, Volatier-Ravat M, Aimez V, Siviloglou G A and Christodoulides D N 2009 *Phys. Rev. Lett.* **103** 093902

[27] Rüter C E, Makris K G, El-Ganainy R, Christodoulides D N, Segev M and Kip D 2010 *Nat. Phys.* **6** 192

[28] Kepesidis K V, Milburn T J, Huber J, Makris K G, Rotter S and Rabl P 2016 *New J. Phys.* **18** 095003

[29] Wu Y, Liu W, Geng J, Song X, Ye X, Duan C K, Rong X and Du J 2019 *Science* **364** 878

[30] Huber J, Kirton P, Rotter S and Rabl P 2020 *SciPost Physics* **9** 052

[31] Nakanishi Y and Sasamoto T 2022 *Phys. Rev. A* **105** 022219

[32] Bender C M and Boettcher S 1998 *Phys. Rev. Lett.* **80** 5243

[33] Bender C M 2007 *Rep. Prog. Phys.* **70** 947

[34] El-Ganainy R, Makris K G, Khajavikhan M, Musslimani Z H, Rotter S and Christodoulides D N 2018 *Nat. Phys.* **14** 11

[35] Moca C P, Sticlet D, Dóra B and Zaránd G 2023 *Phys. Rev. B* **107** 115111

[36] Yan X, Wu H, Fan C, Yang B, Guo Y, Luo X, Xiao J and Zeng Z Y 2025 *Phys. Scri.* **100** 055406

[37] Kattel P, Pasnoori P R and Andrei N 2023 *J. Phys. A: Math. Theor.* **56** 325001

[38] Despres J, Mazza L and Schirò M 2024 *Phys. Rev. B* **110** 094304

[39] Reisenbauer M, Rudolph H, Egyed L, Hornberger K, Zasedatelev A V, Abuzarli M, Stickler B A and Delić U 2024 *Nat. Phys.* **20** 1629

[40] Zhang Y, Carrasquilla J and Kim Y B 2025 *Nat. Commun.* **16** 3286

[41] Kattel P, Zhakenov A, Pasnoori P R, Azaria P and Andrei N 2025 *Phys. Rev. B* **111** L201106

[42] Li Z, Delmonte A, Turkeshi X and Fazio R 2025 *Nat. Commun.* **16** 4329

[43] Rafi-Ul-Islam S M, Siu Z B, Sahin H, Razo M S H and Jalil M B A 2024 *Phys. Rev. B* **109** 045410

[44] Baumann K, Guerlin C, Brennecke F and Esslinger T 2010 *Nature* **464** 1301

[45] Blaß B, Rieger H, Roósz G and Iglói F 2018 *Phys. Rev. Lett.* **121** 095301

[46] Yamamoto K, Nakagawa M, Adachi K, Takasan K, Ueda M and Kawakami N 2019 *Phys. Rev. Lett.* **123** 123601

[47] Hatano N and Nelson D R 1996 *Phys. Rev. Lett.* **77** 570

[48] Sachdev S 2009 *Quantum Phase Transitions* transferred to digital printing ed (Cambridge: Cambridge University Press)

[49] Larson J, Damski B, Morigi G and Lewenstein M 2008 *Phys. Rev. Lett.* **100** 050401

[50] Fernández-Vidal S, De Chiara G, Larson J and Morigi G 2010 *Phys. Rev. A* **81** 043407

[51] Habibian H, Winter A, Paganelli S, Rieger H and Morigi G 2013 *Phys. Rev. Lett.* **110** 075304

[52] Habibian H, Winter A, Paganelli S, Rieger H and Morigi G 2013 *Phys. Rev. A* **88** 043618

[53] Bernardet K, Batrouni G G, Meunier J L, Schmid G, Troyer M and Dorneich A 2002 *Phys. Rev. B* **65** 104519

[54] Jordan P and Wigner E 1928 *Zeitschrift für Physik* **47** 631

[55] Giamarchi T 2003 *Quantum Physics in One Dimension* (Oxford University Press)

[56] Sachdev S 2015 *Quantum Phase Transitions* second edition, 5th edn. (Cambridge: Cambridge University Press)

[57] Altland A and Simons B 2010 *Condensed Matter Field Theory* 2nd edn. (Cambridge; New York: Cambridge University Press)

[58] Moiseyev N 2011 *Non-Hermitian Quantum Mechanics* (Cambridge University Press)

[59] Zhou Y, Kanoda K and Ng T K 2017 *Rev. Mod. Phys.* **89** 025003

[60] Sandvik A W, Avella A and Mancini F 2010 *Computational Studies of Quantum Spin Systems* (Vietri sul Mare, (Italy)) pp. 135–338

[61] Manousakis E 1991 *Rev. Mod. Phys.* **63** 1

[62] Sandvik A W 1997 *Phys. Rev. B* **56** 11678

[63] Li H X, Tan Y, Yang J and Liang B 2023 *Chin. Phys. B* **32** 094301

[64] Li Y, Xing C, Gong M, Guo G and Yuan J 2024 *Chin. Phys. Lett.* **41** 026701

[65] Liu J Y, Wang X Q and Xu Z F 2023 *Chin. Phys. Lett.* **40** 086701